Elsevier Editorial System(tm) for Translational Research

Manuscript Draft

Manuscript Number:

Title: Atrial fibrillation induces preferential myofibroblast differentiation of mesenchymal cardiac progenitor cells.

Article Type: Full Length Article

Keywords: Atrial Fibrillation; mesenchymal cardiac progenitor cells; TGF-β1; myofibroblast; collagen.

Corresponding Author: Dr. Elisa Gambini,

Corresponding Author's Institution:

First Author: Elisa Gambini

Order of Authors: Elisa Gambini; Gabriella Spaltro; Beatrice Bassetti; Gianluca L Perrucci; Giulia Campostrini; Maria Chiara Lionetti; Alberto Pilozzi; Federico Martinelli; Andrea Faruggia; Dario DiFrancesco; Andrea Barbuti; Giulio Pompilio

Manuscript Region of Origin: ITALY

Abstract: Atrial fibrillation (AF) is characterized by electrical, contractile and structural remodeling mediated by interstitial fibrosis. It has been shown that human cardiac mesenchymal progenitor cells (mCPC) can differentiate into endothelial, smooth muscle and fibroblast cells. We have here for the first time investigated the contribution of mCPC in the fibrotic process occurring in AF. As expected, right auricolae samples displayed significantly higher fibrosis in AF vs control (CTR) patients. In tissue samples of AF patients only, double staining for c-kit and the myofibroblast (MFB) marker α-smooth muscle actin (α-SMA) was detected. The number of c-kit positive mCPC was higher in atrial subepicardial regions of CTR than AF. AF-derived mCPC (AF-mCPC) and CTR-derived mCPC (Ctr-mCPC) were phenotypically similar, except for CD90 and c-kit, which were significantly more present in AF and CTR cells, respectively. Moreover, AF showed a lower rate of population-doubling and fold-enrichment vs Ctr-mCPC. When exogenously challenged with the pro-fibrotic growth factor TGF-β1, AF-mCPC showed a significantly higher nuclear translocation of SMAD2 than Ctr-mCPC. In addition, TGF-β1 treatment induced the up-regulation of COL1A1 and COL1A2 in AF-mCPC only. Further, both a marked production of soluble collagen and α-SMA up-regulation has been observed in AF-mCPC only. Finally, electrophysiological studies showed that the inwardly rectifying potassium current IK1 was evenly present in AF and Ctr-mCPC in basal conditions and similarly disappeared after TGF-β1 exposure. All together, these data suggest that AF steers the resident atrial mCPC compartment toward an electrically inert pro-fibrotic phenotype.

April, 21st 2017

Dear Jeffrey Laurence,

We are pleased to submit to your attention the original article entitled: **"Atrial fibrillation induces preferential myofibroblast differentiation of mesenchymal cardiac progenitor cells".**

In this paper, we have studied the contribution of mesenchymal cardiac cells in the process of fibrotic remodeling (mCPC) occurring in atrial fibrillation (AF). Specifically, taking advantage of surgical biopsies, we provided for the first time an evidence that resident mCPC are phenotypically and functionally impacted by the presence of AF, that prompts their differentiation capability towards a pro-fibrotic myofibroblast phenotype. These data suggest that mCPC may be viewed in AF as a contributing cell-player involved in atrial fibrosis onset.

On these basis, we think that this work adds novelty to this topic and may be of interest for the readers of Translational Research.

Sincerely,

Elisa Gambini, PhD

Background

Atrial fibrillation (AF) is characterized by electrical, contractile and structural remodeling, mediated by interstitial fibrosis. It is known that human mesenchymal cardiac progenitor cells (mCPC) can differentiate into cardiomyocyte, fibroblast, endothelial and smooth muscle cells. In vitro and in vivo findings suggest that either an impairment or an alteration of the mCPC compartment is associated with the initiation and progression of cardiomyopathies. The role of mCPC in AF pathogenesis is still unknown.

Translational Significance

Understanding how mCPC are involved in the development of atrial interstitial fibrosis in AF could be important for future investigations on biological therapies influencing AF.

Atrial fibrillation induces preferential myofibroblast differentiation of mesenchymal cardiac progenitor cells.

Elisa Gambini[1#], Gabriella Spaltro[1], Beatrice Bassetti[1], Gianluca Lorenzo Perrucci[1,2], Giulia Campostrini[3], Maria Chiara Lionetti[1], Alberto Pilozzi[4], Federico Martinelli[4], Andrea Faruggia[4], Dario DiFrancesco[3], Andrea Barbuti[3]* and Giulio Pompilio[1,2,4]*.

[1]Vascular Biology and Regenerative Medicine Unit, Centro Cardiologico Monzino IRCCS, Milano
[2]Department of Clinical Sciences and Community Health, Università degli Studi di Milano, Milano
[3]Department of Biosciences, Università degli Studi di Milano, Milano
[4]Department of Cardiovascular Surgery, Centro Cardiologico Monzino IRCCS, Milano.

*Equally contributed
[#]Corresponding author: Elisa Gambini Centro Cardiologico Monzino, Vascular Biology and Regenerative Medicine Unit, Via Parea 4, 20138 Milan, Italy Tel: +390258002027, Fax: +390258002342; email: elisa.gambini@ccfm.it ORCID:orcid.org/0000-0002-8859-8259.

Running title: mCPC involvement in atrial fibrillation.

Abbreviations: AF=atrial fibrillation; TGF-β1=transforming growth factor-β1; mCPC=mesenchymal cardiac progenitor cells; MFB=myofibroblast; α-SMA=α-smooth muscle actin; ECM=extracellular matrix; CTR= controls in sinus rhythm; hrs=hours; BMI=body mass index; α-SA=α-Sarcomeric Actin; HLA=human leucocyte antigen; FACS=flow cytometry; CPD=Cumulative Population doubling; NCX1=sodium-calcium exchanger.

Abstract

Atrial fibrillation (AF) is characterized by electrical, contractile and structural remodeling mediated by interstitial fibrosis. It has been shown that human cardiac mesenchymal progenitor cells (mCPC) can differentiate into endothelial, smooth muscle and fibroblast cells. We have here for the first time investigated the contribution of mCPC in the fibrotic process occurring in AF. As expected, right auricolae samples displayed significantly higher fibrosis in AF *vs* control (CTR) patients. In tissue samples of AF patients only, double staining for c-kit and the myofibroblast (MFB) marker α-smooth muscle actin (α-SMA) was detected. The number of c-kit positive mCPC was higher in atrial subepicardial regions of CTR than AF. AF-derived mCPC (AF-mCPC) and CTR-derived mCPC (Ctr-mCPC) were phenotypically similar, except for CD90 and c-kit, which were significantly more present in AF and CTR cells, respectively. Moreover, AF showed a lower rate of population-doubling and fold-enrichment *vs* Ctr-mCPC. When exogenously challenged with the pro-fibrotic growth factor TGF-β1, AF-mCPC showed a significantly higher nuclear translocation of SMAD2 than Ctr-mCPC. In addition, TGF-β1 treatment induced the up-regulation of COL1A1 and COL1A2 in AF-mCPC only. Further, both a marked production of soluble collagen and α-SMA up-regulation has been observed in AF-mCPC only. Finally, electrophysiological studies showed that the inwardly rectifying potassium current I_{K1} was evenly present in AF and Ctr-mCPC in basal conditions and similarly disappeared after TGF-β1 exposure. All together, these data suggest that AF steers the resident atrial mCPC compartment toward an electrically inert pro-fibrotic phenotype.

Introduction

Atrial fibrillation (AF) is the most common cardiac arrhythmia affecting millions of people worldwide with high mortality and morbidity rates [1]. AF is characterized by a high rate of asynchronous atrial cell depolarization causing a loss of atrial contractile function and irregular ventricular rates [2]. It has been unambiguously reported that atrial fibrosis plays a central role in AF pathogenesis [3]. In this context, transforming growth factor β1 (TGF-β1) is pivotal in the fibrotic process, both in animal models and human, by stimulating myofibroblast (MFB) differentiation and collagen production through the SMAD signaling pathway [4]. Moreover, it has been shown that TGF-β1 expression proportionally increases with the degree of atrial fibrosis in AF [5]. Collagen deposition around cardiomyocytes (interstitial atrial fibrosis) may be the result of non-specific scar-like reparative mechanisms following cardiomyocyte necrosis, being the most threatening change in the setting of atrial structural remodeling in AF [6]. Atrial fibrosis is characterized by the appearance of interstitial MFB. These cells are responsible for the deposition of the extracellular matrix (ECM) that cause cardiomyocyte disarray.

Although major progress has been made in pharmacologic and interventional treatments, persistence and recurrence remain critical problems for AF patients. To date, the exact pathogenic mechanism responsible for AF is still unclear. An improved understanding of the pathophysiology underlying fibrotic atrial remodeling may be relevant for the development of novel therapeutic approaches.

We and others have reported the presence of a resident population of human c-kit$^+$ cardiac mesenchymal progenitor cells (mCPC) [7–10] that can differentiate into endothelial, smooth muscle and, to a lesser extent, fibroblasts [7,8,10,11]. Although the concept that mCPC are cardiomyocyte precursors in the adult heart has been questioned [12], there is enough evidence that this cell population plays anyhow a role in cardiac tissue homeostasis [13,14]. Notably, *in vitro* and *in vivo* findings suggest that either an impairment or an alteration of the mCPC compartment is associated with the initiation and progression of different cardiac conditions [15–18].

Nevertheless, the role and contribution of mCPC in AF pathogenesis, with particular regard to fibrosis and electric dysfunction, is still poorly understood. We have previously shown that AF impairs mCPC amplification potential *ex vivo* [19]. Accordingly, adjunctive evidence has been recently provided that mCPC number is reduced in AF patients, suggesting impairments in self-renewal capability [20].

In the present work, we have investigated the myofibroblastic commitment of human mCPC *vs* controls in sinus rhythm (CTR) obtained from atrial specimens of patients undergoing cardiac surgery. The central message of this study is that AF is associated, *in vitro* and *ex vivo,* with a preferential pro-fibrotic shift of the differentiation program of mCPC.

Material and Methods

Patients and tissue samples

Specimens from right atrial appendages were obtained between May 2012 and January 2014 from 22 Caucasian patients undergoing elective valve surgery. Signed informed consent previously approved by the local ethics committee (R198 – CCFM S202/312) was obtained for each patient in accordance with the declaration of Helsinki. Each tissue sample was divided into 2 parts for mCPC *in vitro* experiments and tissue analyses, respectively. Patients enrolled in this study were allocated into two groups: persistent AF and CTR. In addition to the complete medical record, the following relevant informations were obtained for each patient on admission to the hospital: age, sex, body mass index (BMI), cardiovascular risk factors and drug therapy. Patients were excluded if any of the following criteria were met: i) presence

of coronary artery disease, ii) age > 80 years, iii) positivity for human immunodeficiency virus (HIV), hepatitis B, or hepatitis C, treponema pallidum (VDRL), iv) cardiac surgery in emergency department.

mCPC isolation and culture

The procedure to obtain and expand mCPC from right atrial appendages was carried out as previously reported[7]. Briefly, the myocardial tissue was digested four times at 37°C in a 3 mg/ml collagenase solution (Serva) and cultured in Ham's F12 medium (Lonza) with 10% FBS (Thermo Fisher Scientific), 2 mM L-glutathione and 5 × 10−3 U/mL human erythropoietin (Sigma-Aldrich both), 10 ng/mL bFGF (Peprotech), and antibiotics (Lonza). After a pre-expansion period, cells were stained with APC-conjugated monoclonal antibodies directed against human c-kit receptor (anti-CD117, clone YB5.B8; BD Biosciences), analyzed and sorted by flow cytometry (FACSAria, BD Biosciences). Sorting setup and appropriate gating was established using cells labeled with APC-conjugated isotype control antibody at the same concentration. An appropriate gating strategies has been adopted to selected cells expressing c-kit at high levels only. mCPC were treated with TGF-β1 (2 ng/ml) from 3 hours (hrs) to 10 days to assess differentiation towards the fibroblast lineage. TGF-β1 was added every 48 hrs. In particular, we treated mCPC for: i) 3 hrs to assess SMAD2 nuclear translocation; ii) 48 hrs to analyze collagen gene expression by real time-PCR; iii) 5 days to study the *in vitro* collagen deposition; iv) 10 days to demonstrate *in vitro* myofibroblast differentiation using α-smooth muscle actin (α-SMA) immunofluorescence.

Immunofluorescence and confocal analysis

Fragments from atrial appendages were fixed in paraformaldehyde and processed for tissue inclusion. Sections were de-paraffinized, rehydrated, boiled in antigen retrieval buffer with Na citrate and incubated with primary antibody at 4°C overnight (O/N): c-kit-biotin (Bioss), α-Sarcomeric Actin (α-SA, Sigma-Aldrich), Collagen type I (Coll I, Abcam), α-SMA (Merck Millipore). After washing, sections were incubated with the following fluorochrome-conjugated antibodies for 1 hr at room temperature in the dark: Streptavidin 488 (Life Technologies), DyLight 549 (Jackson Immuno- Research), Alexa 488 (Life Technologies) and Alexa 594 (Life Technologies). Nuclei were stained with Hoechst 33342 (Sigma-Aldrich). Fibrosis was determined by a densitometric analysis of sections stained with a specific antibody to detect Collagen type I and the specific cardiomyocyte marker α-Sarcomeric Actin. The ratio between the number of Coll I pixels (Coll I area sum) and the number of α-SA pixels (α-SA area sum) were calculated with the AxioVision software (Carl Zeiss). In other sections, mCPC niches were identified by an anti-c-kit biotin antibody and by counting c-kit$^+$ cells in 10 random fields. Immunofluorescence was performed at T0 on mCPC untreated or treated with TGF-β1 (2.5 ng/ml), seeded on chamber slides. After washing, mCPC were incubated O/N in the dark, at 4°C with the following antibodies: α-SMA (Merck Millipore) and CD90 (AbCam). The day after, cells were incubated with the following fluorochrome-conjugated antibodies for 1 hr at room temperature in the dark: Alexa 488 and Alexa 633 (Life Technologies both). Nuclei were stained with Hoechst 33342 (Sigma-Aldrich). Analysis was performed using a Zeiss LSM 710 confocal microscope. The number of mCPC were normalized to the section area calculated with ZEN 2008 software (Carl Zeiss) [19].

Flow cytometry

Immunophenotype analysis of mesenchymal, endothelial, human leucocyte antigen (HLA) and hematopoietic markers was performed by multicolor flow cytometry on c-kit$^+$-derived cells. After detachment using a non-enzymatic method, cells were resuspended in PBS containing 0.1% BSA (Gibco, USA) and 2 mM EDTA (Gibco, USA) and incubated in the dark for 15 minutes with suitable combinations of the following monoclonal antibodies or isotype-matched control monoclonal antibodies: c-kit-APC (clone YB5.B8), CD34-FITC (clone 581), CD45-PE (clone HI30), CD29-PE (clone MAR4),

CD31-FITC (clone WM59), CD90-FITC (clone 5E10), CD130-PE (clone AM64), HLA-DR-FITC (clone G46-6), CD73-PE (clone AD2), (BD Pharmingen, Italy), CD146-FITC (clone 128018), CD200-FITC (clone 325516), KDR-PE (clone 89106), (R&D Systems, USA), Lineage-biotin (MiltenyiBiotec, Italy), HLA-G-PE (clone MEM-G/9), (Exbio Praha, Czech Republic), CD144-Alexa700 (clone 16B1, eBioscience, UK). Samples were then washed with 1 mL of washing buffer and centrifuged for 10 minutes at 400 x g at 4°C to remove unbound antibodies. Cells were resuspended in 250 µL of washing buffer and analyzed.

Cumulative population doublings and fold enrichment

Population doubling (PD) levels of mCPC were calculated at every passage in culture, using the following equation: PD = Log N/ Log 2, where N is the number of cells harvested at the end of the culture/the number of seeded cells. Cumulative PD (CPD) was calculated by adding the PD of the passage under analysis to the PD of the previous passages. The fold enrichment of mCPC in culture was calculated as the ratio of the number of c-kit$^+$ cells at passage 3 (P3) / the number of sorted c-kit$^+$ cells at T0 [19].

ImageStreamX assay

Nuclear translocation of SMAD2 in mCPC after TGF-β1 treatment was evaluated by imaging flow cytometry (ImageStream® X Mark II, Amnis). mCPC from CTR patients (Ctr-mCPC) and mCPC from AF patients (AF-mCPC) were cultured in Ham's F12 medium supplemented with 10% FBS and treated with 2.5 ng/ml TGF-β1 (Peprotech) for 3 hrs. After detachment from Petri dishes using a non-enzymatic method, cells were resuspended in 100 µl PBS containing 0.1% BSA (Gibco, USA) and 2 mM EDTA (Gibco, USA) and incubated in the dark for 15 minutes with 0.5 µg/ml anti-SMAD2-FITC primary antibody (AbCam). Samples were then washed with 1 mL per tube of washing buffer and centrifuged for 10 minutes at 400 x g at 4°C to remove unbound antibodies. Cells were resuspended in 100 µL of PBS containing 0.1% BSA and 2 mM EDTA, incubated with 2.5 µM nuclei fluorescent staining DRAQ5 (AbCam), and analyzed. Instrument and INSPIRE software were set up as follows: Ch01 for bright-field, Ch02 for FITC fluorescence intensity, Ch05 for APC fluorescence intensity and Ch06 for side scatter intensity. All samples were acquired with 40X magnification at a low flow rate/high sensitivity and 488, 630 and 785 lasers were activated for FITC fluorescence, APC fluorescence and side-scatter intensity, respectively. mCPC were gated on a dot plot reporting area (x axis) and aspect ratio (y axis) to eliminate clumps. 10,000 events in the mCPC gated area were acquired. Image analysis was performed using the IDEAS image analysis software. The degree of fluorescence relative to SMAD2-FITC staining was quantified using the Intensity_MC_Ch02, while DRAQ5 staining was quantified using the Intensity_MC_Ch05. To evaluate FITC-APC overlapping signal a Similarity Dilate analysis on Intensity_MC_Ch02 and Intensity_MC_Ch05 was performed.

RNA isolation

At P3, before and after culturing in differentiation media (EpiC for cardiac or TGF-β1 for myofibroblastic differentiation), total RNA was purified from mCPC using Trizol reagent (Invitrogen) according to the manufacturer's instructions.

Quantitative reverse transcriptase–polymerase chain reaction (qRT-PCR)

1 µg of total RNA was reverse transcribed (RT) using SuperScriptIII cDNA synthesis kit (Invitrogen, CA). Synthesized cDNA was treated with 2U RNAse H at 37°C for 30 minutes. After reverse transcription, specific primers for early and late cardiac genes, ion channel genes and collagen genes, were used to assess the cell phenotype. Real time q-RT-PCR analysis was performed using iQ5 Real Time PCR System (Bio-Rad, Italy). Each primer pair, designed from available human sequences by using the software Primer Express v3.0 (Applied Biosystems, CA), was tested in triplicate using 10

ng of cDNA. The PCR-reaction included 10 ng of template cDNA, 0.2 μM of each (forward and reverse) primer, 3.5 μl of RNAse-free water and 7.5 μl of iQ SYBR Green Supermix conjugated with the fluorescent dye FAM (Bio-Rad, Italy) in a total volume of 15 μl. Cycling conditions were as follows: 95°C for 10 minutes, followed by 40 amplification cycles of 15 minutes at 95°C for denaturation and 1 minute at 60°C for annealing/elongation. Melting curves were acquired after PCR to confirm the specificity of the amplified products. Quantified values were normalized against the input determined by the housekeeping gene human β-2-microglobulin. Data were expressed and plotted as fold change calculated by normalizing the relative expression (calculated by the 2-ΔΔCt method) to reference cells. In particular, each gene ΔΔCt was calculated on the mean of the ΔCt of the control group (T0). Figure 3 shows the mean of the differences between the threshold cycle (CT) for each amplified transcript and the housekeeping gene (ΔCT), expressed as [(CT target gene)-(CT housekeeping gene)]. Primers pairs used are indicated in Supplementary Table II.

Sircol assay

Total soluble collagen content in cell lysates and supernatant from Ctr-mCPC and AF-mCPC, treated with TGF-β1 for 5 days, was measured using Sircol soluble collagen assays (Biocolor) as described in the manufacturer's protocol. The quantity of collagen was calculated according to a standard curve.

Electrophysiology

Voltage-clamp analyses were performed 3 days after cell sorting (T0 time point), 10 days after TGF-β1 treatment (T10) or 3 weeks after EpiC treatment (T21). For T0 analysis, cells were plated at low density. For the other time points, cells were detached by TrypLE (Life Technologies) and plated at a low density the day before the analysis. Cells were placed onto the stage of an inverted microscope and perfused with the Tyrode solution containing: 140 mM NaCl, 5.4 mM KCl, 1.8 mM CaCl2, 1 mM MgCl2, 5.5 mM D-glucose, 5 mM Hepes-NaOH; pH 7.4. Patch-clamp pipettes were filled with an intracellular-like solution containing: 130 mM K-aspartate, 10 mM NaCl, 5 mM EGTA-KOH, 2 mM $CaCl_2$, 2 mM $MgCl_2$, 2 mM ATP (Na-salt), 5 mM phosphocreatine, 0.1 mM GTP (Na-salt), 10 mM Hepes-KOH; pH 7.2. Cells were kept at room temperature. I_{K1} current was recorded from single cells in whole-cell configuration as the Ba^{2+}-sensitive component following a 200 ms voltage ramp from -100 to 0 mV (holding potential, hp-60 mV). Current density was obtained normalizing the Ba^{2+}-sensitive current for the cell capacitance. The fast Na+ current (I_{Na}) was activated by 30 ms steps to the range -80/+10 mV from a hp of -90 mV. the I_f was recorded applying a single voltage step to -115 mV (hp -30 mV) in tyrode solution with, 1 mM $BaCl_2$ and 2 mM $MnCl_2$ to in order to block contaminating currents.

Statistical analysis

Quantitative results are expressed as mean ± SD. Variables were analyzed by Student's t test. Statistical significance was evaluated with GraphPad Prism 5 and a value of $p \leq 0.05$ was considered as statistically significant.

Results

Patient characteristics

A total of 22 cardiac specimens (right atrial appendages) from patients undergoing isolated aortic (n=13), or combined mitral-tricuspid (n=6), aortic-tricuspid (n=1) or aortic-mitral-tricuspid (n=2) valve surgery, showing permanent AF (AF group; n=11), or sinus rhythm (CTR group; n=11) were analyzed. Details of patient characteristics are shown in Table 1.

The two groups were matched for age and gender. Cardiovascular risk factors and medication profile were also similar in both groups. As expected, the vast majority of AF patients underwent mitral and tricuspid valve surgery (p<0.01) while CTR patients aortic valve surgery (p<0.01).

Tissue characterization and mCPC localization

Increased collagen deposition has been well documented in AF patients compared with CTR subjects [21]. Using a densitometric analysis, we found that right auricolae fragments recapitulated left atrial fibrotic remodeling in AF patients (Fig 1, A and B), showing significantly higher fibrosis *vs* CTR patients (p<0.001, n=3, Fig 1C). By immunofluorescence analysis, the presence of isolated or clustered c-kit$^+$ cells in subepicardial or subendocardial zones has been detected (Fig 1, D-G). Of note, mCPC number was found to be significantly higher in the subepicardial region of CTR than in AF patients (p<0.05, n=3) and not different in the subendocardial territory (Fig 1H). To preliminary test at tissue level a possible involvement of mCPC as cellular origin of MFB, we checked for c-kit cells co-expressing α-SMA in AF and CTR tissue samples. Of interest, double-positive c-kit/α-SMA cells have been observed in AF samples only (Fig 1, I and L).

mCPC isolation and amplification

Cardiac tissue samples were processed for mCPC isolation (purity >80%) and *in vitro* assays. AF-mCPC were characterized by a lower rate of population doubling (p<0.05, n=7) and fold-enrichment (p<0.05, n=5) compared to Ctr-mCPC (Fig 2, A and B), in agreement with our previously reported data [19]. AF-mCPC and Ctr-mCPC showed a similar percentage of positivity for surface antigens typical of mesenchymal cells (Supp. Table I), however c-kit (CD117) and CD90 (Thy-1) were significantly higher in Ctr-mCPC and AF-mCPC, respectively (p<0.05, n=6) (Fig 2, C and D).

In vitro effects of TGF-β1 treatment on mCPC

To study whether a fibrotic commitment may be triggered in the mCPC population, AF and Ctr-mCPC have been exposed to TGF-β1 to evaluate the nuclear translocation of SMAD2, a downstream transcription factor involved in the TGF-β1 pathway. Although TGF-β1 treatment induced the nuclear translocation of SMAD2 in both cell types, the differences between nuclear localization of SMAD2 before and after TGF-β1 treatment (Δ similarity dilate cell percentage) was significantly higher in AF-mCPC than Ctr-mCPC (11.08 ± 0.38 *vs* 17.68 ± 0.33, p<0.001) (Fig 3, A and B). This assay was performed with ImageStream® X flow cytometer, which combines flow cytometry with confocal microscopy technology. Although it has already been shown that TGF-β1 activates SMAD2 translocation to the nucleus thus activating its down-stream pathway, we demonstrated for the first time such an over-activation in human mCPC and a preferential activation in AF-mCPC.

Further, to analyse the differentiation ability of mCPC into MFB, we took advantage of different assays at various time points to follow such progression. Specifically, i) after 48 hrs of TGF-β1 treatment, we showed the up-regulation of COL1A1 (p<0.05) and COL1A2 (p<0.01) genes in AF-mCPC only; on the contrary, COL3A1 gene expression was up-regulated in Ctr-mCPC only at the same time point (p<0.01) (Fig 3C); ii) after 5 days of TGF-β1 treatment, we found a significant production of soluble collagen, as detected by Sircol assay, in AF samples only (5.64±1.58 in AF-mCPC *vs* 2.34±0.54 in Ctr-mCPC, p<0.05; n=4), (Fig 4A); iii) as a confirmation of the mCPC in MFB and as further evidence of SMAD2 activation, a significant α-SMA up-regulation was observed in AF-mCPC by immunofluorescence analysis after 10 days of TGF-β1 treatment (Fig 4, B and C).

mCPC gene expression after TGF-β1 treatment

To evaluate the early mCPC cardiogenic commitment, qPCR for early cardiac markers was performed at T0 and after 10 days of TGF-β1 exposure in both groups. Interestingly, we observed at baseline a significant higher expression of early cardiac genes (GATA-4, Nkx2.5, HAND-2 and TBX5) in AF-mCPC than in Ctr-mCPC ($p<0.05$) followed by a significant decrease after TGF-β1 exposure in AF-mCPC only (Suppl. Fig 1A). We also checked the expression of different ion channel genes (Suppl. Table 2) at T0 and after 10 days of TGF-β1 treatment. We detected no variation in the genes analyzed between Ctr- and AF-mCPC with the exception of NCX1, that was significantly down-regulated in both groups after TGF-β1 treatment, and of CACNA1C and Kv4.3, that were significantly up-regulated in Ctr-mCPC only after TGF-β1 treatment (Suppl Fig 1B). Notably, Kir2.1 gene expression was significantly down-regulated in both groups after TGF-β1 treatment (Fig 5A).

mCPC electrophysiological studies

Given the previously reported implication of potassium channels variations with collagen deposition in fibroblasts [22], we performed electrophysiological studies in AF and Ctr-mCPC before (T0) and after TGF-β1 treatment to study the I_{K1} current. The cell capacitance was significantly higher in both groups after TGF-β1 treatment, and Ctr-mCPC showed higher cell capacitance *vs* AF-mCPC in basal conditions and after TGF-β1 treatment (Fig 5B). In agreement with Kir2.1 mRNA data shown in Fig 5A, both AF- and Ctr-mCPC at T0 similarly expressed a Ba^{2+}-sensitive I_{K1} current (Ctr-mCPC -2.2±0.4 pA/pF, AF-mCPC -2.3±0.5 pA/pF), that almost disappeared after TGF-β1 exposure (Fig 5C, D).

Since HCN4 mRNA and mRNA of the sodium channel Nav1.5 is expressed in Ctrl and AF-mCPC at basal level (T0), we have also evaluated the I_f (carried by HCN4) and I_{Na} (carried by Nav1.5) currents at T0. We never recorded I_f in both cell groups; I_{Na} was recorded in one control- and one AF-mCPC out of 19 and 21 cell analyzed, respectively (data not shown).

Discussion

In this study, we have reported for the first time that the differentiation program of mesenchymal c-kit$^+$ cardiac atrial cells undergoes a pro-fibrotic shift in the presence of AF. Specifically, we have shown that resident mCPC taken from the right atrium of AF patients are fewer and show a diminished expansion capability with respect to those isolated from patients in sinus rhythm. More importantly, AF-derived cardiac progenitors can preferentially differentiate at tissue level and *in vitro* into MFB triggering reactive collagen deposition. Finally, we have found that AF-derived mCPC do not show differences versus Ctr-mCPC in k(+)-dependent channel genes and relative functional patterns.

Recently, Shinohara D and coworkers [20] have reported that the ratio of c-kit$^+$ cells contained in outgrowth cells from left atrial tissue did not increase in the presence of AF and that both the total number of outgrown cells and the number of c-kit positive cells after 28 days of *in vitro* expansion were decreased in AF group with respect of sinus rhythm controls. The authors inferred from these results that CPC impairment in self-renewal might concur with a diminished healing capability of AF atrial tissue upon remodeling injury. Our results confirmed that c-kit$^+$ mCPC are significantly less abundant in atrial tissue of AF compared to CTR patients, being such a reduction observed in the subepicardial region only, whereas no differences have been detected at the endocardial level. This finding is in agreement with the previously reported data on the relatively small contribution of endocardial cells to the adult heart interstitial fibroblast compartment [23]. Moreover, we have found that mCPC obtained from AF patients were characterized in culture by a lower rate of fold-enrichment compared to mCPC derived from patients in sinus rhythm, as well as by an impairment of the cumulative population doubling. This evidence parallels our previous finding of a robust negative

association between AF and *in vitro* mCPC proliferation [19] and concurs with Shinohara's [20] findings. Whether such a proliferation impairment is due to a cell exhaustion process or to an enhanced differentiation commitment, this is at present a matter of mere speculation and deserves further investigation.

To date, anyhow, no adjunctive information is available in the literature about the relative contribution of the mCPC compartment to develop atrial structural damage in AF. The critical association between AF, reactive interstitial fibrosis and ECM deposition leading to atrial remodeling is well established [24]. Fibrosis is now viewed as the disease process that triggers the initiation and maintenance of AF [25]. Increased collagen deposition is present in patients with AF secondary to mitral valve disease versus those in sinus rhythm [26], since extracellular matrix volume and composition is in direct correlation with AF persistence [27]. Notably, although these findings highlight the association between atrial fibrosis and AF, the demonstration of a causal relationship of ECM deposition in AF occurrence and persistence remains an important challenge [28]. Mechanistically, converging data implicate the crucial role of pro-fibrotic molecules downstream of the angiotensin axis such as TGF-β1 in the development of atrial fibrotic structural remodeling [29].

The principal cellular effectors of reactive interstitial fibrosis are MFB, which appear in the myocardium following pathological conditions. The most reliable marker for MFB is α-SMA which is expressed in smooth-muscle cells but not in fibroblasts. MFB are the main producers of ECM, critically contributing to reactive cardiac fibrosis [30,31], being TGF-β1 the main molecular driver of their role in fibrotic process [32]. Notably, even though MFB share phenotypic properties with fibroblasts and smooth-muscle cells, their precise origin is not fully resolved, and remains an area of active research [33,34]. Although MFB are generally believed to be derived through the activation of resident cardiac fibroblasts, this view has been challenged by the demonstration of phenotypic heterogeneity among mesenchymal-derived fibroblast populations [23,35], not only between organs, but also within the same organ during health and disease [36,37].

We have previously characterized resident c-kit$^+$ mCPC as a cell population expressing typical mesenchymal markers [7]. Although the cardiomyogenic potential of c-kit$^+$ mCPC in adulthood has been questioned [12], there is enough evidence so far indicating that resident c-kit$^+$ mCPC present in the adult heart possess a mesenchymal phenotype and are capable of contributing significantly to non-myocardial lineages (fibroblasts, smooth muscle cells, and endothelial cells) [11,38,39]. Moreover, mCPC have been described to play a role in physiologic cardiac homeostasis and in the pathogenesis of various cardiac conditions, including myocardial infarction and cardiomyopathies [15,40,41].

We have previously shown for the first time that the presence of AF impairs atrial mCPC amplification potential *ex vivo* [19]. As an additional finding, this study suggest that, when appropriately stimulated, mCPC obtained from right atrial tissue of AF patients are shifted toward a preferential MFB commitment when compared to mCPC from sinus rhythm counterparts. Specifically, after TGF-β1 treatment, AF-mCPC showed with respect to Ctr-mCPC: i) an increased SMAD2 nuclear translocation, which is known to regulate, through TGF-β1 pathway [42], the transcription of pro-fibrotic target genes; ii) an increased *in vitro* expression of the specific MFB marker α-SMA, together with a substantial loss of CD90; iii) an increased capacity of collagen production. In particular, collagen upregulation in TGF-β1 treated AF-mCPC has been confirmed in our experiments at both transcript and protein levels. Major components of ECM are collagen type I, which is produced by cardiac fibroblasts and accounts for about 80% of collagen in the whole heart tissue, and type III, which is preferentially found in the myocardium [43,44]. The most detrimental event in the interstitial fibrotic process is the deposition of the thicker type I collagen, which confers an increased stiffness to the cardiac tissue [45] and is involved in different pathological conditions [46], including AF. Of note, upon TGF-β1 stimulation both transcripts of the two main collagen I isoforms were found to be more significantly increased in AF *vs* Ctr-mCPC. As further evidence, the well-known mesenchymal surface marker CD90 was the only among many we identified to be significantly more expressed in AF-mCPC than Ctr, as shown in Figure 2D and Figure 4B, C. Since, as previously described [47], CD90 has been used as positive control for fibroblasts in various organs, such a distinct distribution of the Thy-1 protein observed in our AF *vs*

Ctr-mCPC populations provides an additional confirmation of a shift of the differentiation program of AF-mCPC into a fibroblastic commitment.

Intriguingly, a broad basal difference between AF and CTR was revealed in the expression of a core cardiac transcriptional network, with particular regard to four genes distinctive of early cardiac commitment (Nkx2.5, Gata-4, TBX-5 and Hand-2). The potential early cardiac plasticity of cardiac mesenchymal-derived cells is not surprising. Furtado and coworkers [23] have reported that a plethora of early cardiac genes were all significantly upregulated in sub-populations of cardiac fibroblasts compared with tail fibroblasts. Moreover, there is robust evidence that c-kit$^+$ cardiac progenitors may show early cardiomyocyte markers [13]. Interestingly, our unprecedented findings indicate that the primary AF-mCPC population is more primed for myogenic transdifferentiation at basal level compared with Ctr-mCPC, and that this difference is suppressed by TGF-β1 stimulation. Although we do not have a clear explanation for these data, one can speculate that an initial cardiogenic response of mCPC to atrial tissue damage occurring in AF cannot be sustained once the fibrotic stimulus is established.

Besides the concept that reactive interstitial fibrosis contributes to cardiac arrhythmias by affecting passive properties of impulse conduction, recent studies demonstrated that fibroblasts and MFB may play an active arrythmogenic role in AF driving inward current for cardiac impulse conduction, and therefore generating an arrhythmogenic uniformly slow propagation [28]. Cardiac fibroblasts are well known to possess a range of ion channels, although their functional roles are still poorly characterized. It has been recently demonstrated that the upregulation of the background inward-rectifier potassium current (I_{K1}) in atrial fibroblasts from chronic heart failure hearts may play a role in promoting fibroblast remodeling and structural/arrhythmic alterations [48]. Moreover, Zhang YY and coworkers [49] have recently reported the existence of several ionic currents in human cardiac c-kit$^+$ progenitors such as the inwardly rectifying K^+ current, present in 84% of cells. We then sought to investigate the ion channels and arrhythmic profile of AF- *vs* Ctr-mCPC in both basal and TGF-β1 stimulated conditions. Of interest, no basal differences were found as for multiple ion channel genes in AF *vs* CTR. In both cell types, TGF-β1 exposure led to a significant down-regulation of the sodium-calcium exchanger (NCX1) and, of the Kir2.1 inward-rectifier potassium ion channel. Notably, patch-clamp recording showed a suppression of the I_{k1} current upon TGF-β1 stimulation in both Ctr and AF-mCPC. These findings may have implications as for mCPC profile in AF. First, AF-mCPC Kv-channel genes down-regulation may play a pro-fibrotic role in AF substrate, as previously demonstrated in canine atrial fibroblasts [22]. Second, the lack of difference between AF *vs* Ctr-mCPC in k(+)-dependent channel genes and relative functional patterns at both basal and pro-fibrotic conditions suggests that mCPC may not play an active role in AF electric atrial remodeling.

All together, we believe these data are supportive for a contributive role of the mCPC population to the development of atrial interstitial fibrosis in AF. Although resident mCPC have reported by us and others to be scarcely represented within the whole mesenchymal stromal compartment [50], their involvement in collagen deposition may be nevertheless not negligible and remains to be clarified.

Limitations. We acknowledge that study specimens have been obtained from the right atrium only. However, the concordance of published *in vitro* data reported with mCPC from left atrial appendages [20] is reassuring as to the reliability of our results. Second, we are well aware that, as previously mentioned [39], it is theoretically possible that *in vitro* conditions may increase or shift the differentiation capacity of mCPC cells from certain lineages to others, whereas in the *in vivo* setting environmental signals may limit this phenomenon, even in response to injury. However, we believe that the multiple pieces of evidence we have collected in this work are convincing as for a fibrotic commitment of AF-mCPC versus controls. Finally, we do not have an explanation for differences observed in cell capacitance of AF-mCPC *vs* sinus rhythm controls.

Conclusion. Cumulatively, our data suggest that resident mCPC are impacted in number and function by AF, which steers their differentiation capability towards a myofibroblast pro-fibrotic phenotype. On the contrary, no evidence has been collected as to differences between AF- and Ctr-mCPC in the elecrophysiological profile.

Acknowledgments

This work was supported by Centro Cardiologico Monzino IRCCS, RC 2014/15 end RC 2015/16. The authors declare no competing financial interests. We are thankful to Aoife Gowran, PhD for revising the manuscript.

Bibliography

1. Hu Y-F, Chen Y-J, Lin Y-J, Chen S-A. Inflammation and the pathogenesis of atrial fibrillation. *Nat Rev Cardiol*. 2015;12(4):230-243. doi:10.1038/nrcardio.2015.2.

2. Aimé-Sempé C, Folliguet T, Rücker-Martin C, et al. Myocardial cell death in fibrillating and dilated human right atria. *J Am Coll Cardiol*. 1999;34(5):1577-1586. doi:10.1016/S0735-1097(99)00382-4.

3. Li D, Fareh S, Leung TK, Nattel S. Promotion of atrial fibrillation by heart failure in dogs: atrial remodeling of a different sort. *Circulation*. 1999;100(1):87-95. doi:10.1161/01.CIR.100.1.87.

4. Khan R, Sheppard R. Fibrosis in heart disease: Understanding the role of transforming growth factor-β1 in cardiomyopathy, valvular disease and arrhythmia. *Immunology*. 2006;118(1):10-24. doi:10.1111/j.1365-2567.2006.02336.x.

5. Xiao H, Lei H, Qin S, Ma K, Wang X. TGF-??1 expression and atrial myocardium fibrosis increase in atrial fibrillation secondary to rheumatic heart disease. *Clin Cardiol*. 2010;33(3):149-156. doi:10.1002/clc.20713.

6. Corradi D. Atrial fibrillation from the pathologist's perspective. *Cardiovasc Pathol*. 2014;23(2):71-84. doi:10.1016/j.carpath.2013.12.001.

7. Gambini E, Pompilio G, Biondi A, et al. C-kit+ cardiac progenitors exhibit mesenchymal markers and preferential cardiovascular commitment. *Cardiovasc Res*. 2011;89(2):362-373. doi:10.1093/cvr/cvq292.

8. Oh H, Bradfute SB, Gallardo TD, et al. Cardiac progenitor cells from adult myocardium: homing, differentiation, and fusion after infarction. *Proc Natl Acad Sci U S A*. 2003;100(21):12313-12318. doi:10.1073/pnas.2132126100.

9. Beltrami AP, Barlucchi L, Torella D, et al. Adult cardiac stem cells are multipotent and support myocardial regeneration. *Cell*. 2003;114(6):763-776. doi:10.1016/S0092-8674(03)00687-1.

10. Smith RR, Barile L, Cho HC, et al. Regenerative potential of cardiosphere-derived cells expanded from percutaneous endomyocardial biopsy specimens. *Circulation*. 2007;115(7):896-908. doi:10.1161/CIRCULATIONAHA.106.655209.

11. Fuentes T, Kearns-Jonker M. Endogenous cardiac stem cells for the treatment of heart failure. *Stem Cells Cloning Adv Appl*. 2013;6(1):1-12. doi:10.2147/SCCAA.S29221.

12. van Berlo JH, Kanisicak O, Maillet M, et al. C-Kit+ Cells Minimally Contribute Cardiomyocytes To the Heart. *Nature*. 2015;509(7500):337-341. doi:10.1038/nature13309.

13. Bearzi C, Rota M, Hosoda T, et al. Human Cardiac Stem Cells. *Proc Natl Acad Sci*. 2007;104(35):14068-14073. doi:10.1073/pnas.0706760104.

14. Johnston P V., Sasano T, Mills K, et al. Engraftment, differentiation, and functional benefits of autologous cardiosphere-derived cells in porcine ischemic cardiomyopathy. *Circulation*. 2009;120(12):1075-1083. doi:10.1161/CIRCULATIONAHA.108.816058.

15. De Angelis A, Piegari E, Cappetta D, et al. Anthracycline cardiomyopathy is mediated by depletion of the cardiac stem cell pool and is rescued by restoration of progenitor cell function. *Circulation*. 2010;121(2):276-292. doi:10.1161/CIRCULATIONAHA.109.895771.

16. Katare R, Oikawa A, Cesselli D, et al. Boosting the pentose phosphate pathway restores cardiac progenitor cell availability in diabetes. *Cardiovasc Res*. 2013;97(1):55-65. doi:10.1093/cvr/cvs291.

17. Avolio E, Gianfranceschi G, Cesselli D, et al. Ex vivo molecular rejuvenation improves the therapeutic

activity of senescent human cardiac stem cells in a mouse model of myocardial infarction. *Stem Cells*. 2014:2373-2385. doi:10.1002/stem.1728.

18. Spaltro G, Avitabile D, Falco E De, Gambini E. Physiological conditions influencing regenerative potential of stem cells. 2016:1126-1150.

19. Gambini E, Pesce M, Persico L, et al. Patient profile modulates cardiac c-kit+ progenitor cell availability and amplification potential. *Transl Res*. 2012;160(5):363-373.

20. Shinohara D, Matsushita S, Yamamoto T, et al. Reduction of c-kit positive cardiac stem cells in patients with atrial fibrillation. *J Cardiol*. 2016. doi:10.1016/j.jjcc.2016.07.006.

21. Anter E, Callans DJ. Pharmacological and electrical conversion of atrial fibrillation to sinus rhythm is worth the effort. *Circulation*. 2009;120(14):1436-1443. doi:10.1161/CIRCULATIONAHA.108.824847.

22. Wu CT, Qi XY, Huang H, et al. Disease and region-related cardiac fibroblast potassium current variations and potential functional significance. *Cardiovasc Res*. 2014;102(3):487-496. doi:10.1093/cvr/cvu055.

23. Furtado MB, Costa MW, Pranoto EA, et al. Cardiogenic genes expressed in cardiac fibroblasts contribute to heart development and repair. *Circ Res*. 2014;114(9):1422-1434. doi:10.1161/CIRCRESAHA.114.302530.

24. Smaill BH. Fibrosis, Myofibroblasts, and Atrial Fibrillation. *Circ Arrhythmia Electrophysiol*. 2015;8(2):256-257. doi:10.1161/CIRCEP.115.002881.

25. Gal P, Marrouche NF. Magnetic resonance imaging of atrial fibrosis : redefining atrial fibrillation to a syndrome. 2017:14-19. doi:10.1093/eurheartj/ehv514.

26. Boldt A, Wetzel U, Lauschke J, et al. Fibrosis in left atrial tissue of patients with atrial fibrillation with and without underlying mitral valve disease. *Heart*. 2004;90(4):400-405. doi:10.1136/hrt.2003.015347.

27. Xu J, Cui G, Esmailian F, et al. Atrial Extracellular Matrix Remodeling and the Maintenance of Atrial Fibrillation. *Circulation*. 2004;109(3):363-368. doi:10.1161/01.CIR.0000109495.02213.52.

28. Miragoli M, Glukhov A V. Atrial Fibrillation and Fibrosis: Beyond the Cardiomyocyte Centric View. *Biomed Res Int*. 2015;2015:798768. doi:10.1155/2015/798768.

29. Polejaeva IA, Ranjan R, Davies CJ, et al. Increased Susceptibility to Atrial Fibrillation Secondary to Atrial Fibrosis in Transgenic Goats Expressing Transforming Growth Factor-??1. *J Cardiovasc Electrophysiol*. 2016;27(10):1220-1229. doi:10.1111/jce.13049.

30. Eghbali M, Weber KT. Collagen and the myocardium: fibrillar structure, biosynthesis and degradation in relation to hypertrophy and its regression. *Mol Cell Biochem*. 1990;96(1):1-14. doi:10.1007/BF00228448.

31. Carver W, Terracio L BT. Expression and accumulation of interstitial collagen in the neonatal rat heart. *Anat Rec*. 1993;236(3):511-520.

32. Juan F. SANTIBANEZ ˜ MQ and CB. TGF-β/TGF-β receptor system and its role in physiological and pathological conditions. *Clin Sci*. 2011;121:233-251. doi:10.1042/CS20110086.

33. Hinz B, Phan SH, Thannickal VJ, Galli A, Bochaton-Piallat M-L, Gabbiani G. The Myofibroblast. *Am J Pathol*. 2007;170(6):1807-1816. doi:10.2353/ajpath.2007.070112.

34. Wynn T a, Yugandhar VG, Clark M a. Cellular and molecular mechanisms of fibrosis. *J Pathol*. 2013;46(2):26-32. doi:10.1002/path.2277.Cellular.

35. Chang HY, Chi J-TJ, Dudoit S, et al. Diversity, topographic differentiation, and positional memory in

human fibroblasts. *Proc Natl Acad Sci*. 2002;99(20):12877-12882. doi:10.1073/pnas.162488599.

36. Fries KM, Blieden T, Looney RJ, et al. Evidende for fibroblast heterogenity and the role of fibroblast subpopulations in fibrosis. *Clin Immunol Immunopathol*. 1994;72(3):283-292. doi:10.1006/clin.1994.1144.

37. Jelaska a, Strehlow D, Korn JH. Fibroblast heterogeneity in physiological conditions and fibrotic disease. *Springer Semin Immunopathol*. 1999;21(4):385-395. doi:10.1007/s002810000032.

38. Ellison GM, Vicinanza C, Smith AJ, et al. Adult c-kitpos cardiac stem cells are necessary and sufficient for functional cardiac regeneration and repair. *Cell*. 2013;154(4):827-842. doi:10.1016/j.cell.2013.07.039.

39. Keith MCL, Bolli R. "string theory" of c-kitpos cardiac cells: A new paradigm regarding the nature of these cells that may reconcile apparently discrepant results. *Circ Res*. 2015;116(7):1216-1230. doi:10.1161/CIRCRESAHA.116.305557.

40. Tallini YN, Greene KS, Craven M, et al. C-Kit Expression Identifies Cardiovascular Precursors in the Neonatal Heart. *Proc Natl Acad Sci U S A*. 2009;106(6):1808-1813. doi:0808920106 [pii]\r10.1073/pnas.0808920106.

41. Nigro P, Perrucci GL, Gowran A, Zanobini M, Capogrossi MC, Pompilio G. C-kit^{+} cells: The tell-tale heart of cardiac regeneration? *Cell Mol Life Sci*. 2015;72(9):1725-1740. doi:10.1007/s00018-014-1832-8.

42. Inman GJ, Nicolás FJ, Hill CS. Nucleocytoplasmic shuttling of Smads 2, 3, and 4 permits sensing of TGF-beta receptor activity. *Mol Cell*. 2002;10:283-294. doi:S1097276502005853 [pii].

43. Swynghedauw B, National I, Sante D. Molecular Mechanisms of Myocardial Remodeling. 1999;79(1):215-262.

44. Lijnen PJ, Petrov V V, Fagard RH. Induction of Cardiac Fibrosis by Transforming Growth Factor- ␣ 1. 2000;435:418-435. doi:10.1006/mgme.2000.3032.

45. Poulsen SH, Host NB, Jensen SE, Egstrup K. Relationship between serum amino-terminal propeptide of type III procollagen and changes of left ventricular function after acute myocardial infarction. *Circulation*. 2000;101(13):1527-1532. doi:10.1161/01.CIR.101.13.1527.

46. Jugdutt BI. Ventricular remodeling after infarction and the extracellular collagen matrix: When is enough enough? *Circulation*. 2003;108(11):1395-1403. doi:10.1161/01.CIR.0000085658.98621.49.

47. Ieda M, Tsuchihashi T, Ivey KN, et al. Cardiac Fibroblasts Regulate Myocardial Proliferation through ??1 Integrin Signaling. *Dev Cell*. 2009;16(2):233-244. doi:10.1016/j.devcel.2008.12.007.

48. Qi XY, Huang H, Ordog B, et al. Fibroblast inward-rectifier potassium current upregulation in profibrillatory atrial Remodeling. *Circ Res*. 2015;116(5):836-845. doi:10.1161/CIRCRESAHA.116.305326.

49. Zhang Y-Y, Li G, Che H, et al. Characterization of functional ion channels in human cardiac c-kit+ progenitor cells. *Basic Res Cardiol*. 2014;109(3):407. doi:10.1007/s00395-014-0407-z.

50. Itzhaki-Alfia A, Leor J, Raanani E, et al. Patient characteristics and cell source determine the number of isolated human cardiac progenitor cells. *Circulation*. 2009;120(25):2559-2566. doi:10.1161/CIRCULATIONAHA.109.849588.

Table and Figure legends

Table 1. Clinical characteristics of patients included in the study

Figure 1. Tissue collagen deposition and mCPC localization. Representative images of human right atrial appendage longitudinal section from CTR **(A)** and AF **(B)** patients immunostained with Collagen type I (Coll I) and α-Sarcomeric Actin (α-SA). Nuclei were stained with Hoechst 33258 (blue) **(C)** Mean bar graph of the ratio of the densitometric analysis of the area stained by Coll I and α-SA. Data showed the average of four images and were representative of three independent experiments. ***p< 0.001 n=3. Representative images of right atrial appendages subepicardial regions of CTR **(D)** and AF **(E)** patients immunostained with c-kit and α-Sarcomeric Actin (α-SA) antibody. Representative images of right atrial appendages subendocardial regions of CTR **(F)** and AF **(G)** patients immunostained with c-kit and α-Sarcomeric Actin (α-Sarc) antibody. In all sections, nuclei were stained with Hoechst 33258 **(H)** mCPC niche quantitative estimation. The number of c-kit$^+$ cells from 10 randomly selected fields were counted for each tissue section of AF and CTR patients. At subepicardial regions c-kit$^+$ cells are significantly more abundant in CTR compare to AF patients *p<0.05. Data were representative of three independent experiments. Representative images of human right atrial appendage section from CTR **(I)** and AF **(L)** patients immunostained with a-SMA (red) and c-kit (green). In CTR section c-kit$^+$ cells did not express α-SMA and identify vessels. In AF sample c-kit$^+$ cells co-express α-SMA (see arrows) and are present also in region far from the vessels. Nuclei were stained with Hoechst 33258 (blue) *=p<0.05, ***p< 0.001 n=3.

Figure 2. *In vitro* properties of human mCPC. (A) Cumulative Population Doubling (PD) of mCPC in culture. *p<0.05 n=7. **(B)** Fold enrichment of mCPC in culture. *p<0.05, n=5. **(C-D)** Mean bar graph of the expression of **(C)** c-kit and **(D)** CD90 markers by Flow Cytometry.*=p<0.05 n=6.

Figure 3. Transcriptional effect *in vitro* mCPC after TGF-β1 treatment. (A) Results obtained by ImageStream® X (IMX),on SMAD2 nuclear translocation in Ctr-mCPC and AF-mCPC before and after 3 h of TGF-β1 (2 ng/ml) treatment IMX microscopy images of fixed mCPC, hybridized with anti-SMAD2-FITC antibody (green) and stained with DRAQ5 for the nucleus (red). Merged signal (yellow) indicates SMAD2 nuclear translocation in AF-mCPC after TGF-β1 treatment. **(B)** IMX FACS analysis on data collected from 10,000 events (per sample). The histograms summarize the differences between positive Similarity dilate cell percentage of Ctr-mCPC (white bar) and AF-mCPC (black bar), before and after TGF-β1 treatment. Among AF-mCPC, the number of cells showing nuclear translocation of SMAD2 signal results significantly higher than Ctr-mCPC (11.08 ± 0.38 *vs* 17.68 ± 0.33, p<0.001). **(C)** qPCR expression analysis of collagen genes Col 1A1, Col 1A2 and Col 3A1 expressed in Ctr-mCPC and AF-mCPC treated with TGF-β1 for 48 hrs. Fold increase was calculated by the $2^{-\Delta\Delta Ct}$ method and normalized by the expression of each genes at T0 (T0=F12 hrs; 48 hrs=F12h+TGFβ 2 ng/mL 48 hrs). *** p < 0.001 in Ctr-mCPC *vs* AF-mCPC, n=3. # p < 0.05 in AF-mCPC T0 *vs* TGF-β1, ## p < 0.01 in AF-mCPC T0 *vs* TGF-β1, §§ p < 0.01 in Ctr-mCPC T0 *vs* TGF-β1, n=4.

Figure 4. Effects of TGF-β1 treatment in myofibroblast differentiation of mCPC *in vitro* (A) Sircol assay to assess the expression of soluble collagen by Ctr-mCPC and AF-mCPC treated with TGF-β1 for 5 days. **(B)** Representative images of immunofluorescence experiments on Ctr-mCPC and AF-mCPC for CD90 (green) and a-SMA (red). Nuclei are stained with Hoechst 33258. **(C)** Densitometric analysis of the ratio between α-SMA and CD90 fluorescence intensity. Data showed the average of three images and were representative of three independent experiments.

Figure 5. mCPC electrophysiological studies: (A) Quantification of Kir2.1 gene expression in Ctr-mCPC and AF-mCPC in basal condition (T0) and after 10 days in TGF-β1 treatment (TGF-β1). # p < 0.05 in AF-mCPC T0 *vs* TGF-β1, § p < 0.05 in Ctr-mCPC T0 *vs* TGF-β1, n=5. **(B)** Bar graph of the Mean Cell Capacitance (MCC) in basal conditions (T0) and after 10 days in TGF-β1 treatment (TGF-β1). * p < 0.05, ** p < 0.01 in Ctr-mCPC *vs* AF-mCPC, ## p < 0.01 in AF-mCPC T0 *vs* TGF-β1, §§ p < 0.01 in Ctr-mCPC T0 *vs* TGF-β1, n=11. **(C)** representative I_{K1} recordings from CTR- and AF-mCPC in basal condition (T0) and after 10 days in TGF-β1 treatment (TGF-β1) before and after perfusion of 2 mM Ba^+. **(D)** Mean current-voltage relation of the Ba^+-sensitive I_{K1} current. At T0 (Ctr-mCPC -2.2±0.4 pA/pF, AF-mCPC -2.3±0.5 pA/pF at -100 mV and after TGF-β1 treatment for 10 days (Ctr-mCPC -0.17±0.22, pA/pF n=8, AF-mCPC -0.26±0.67 pA/pF n=6, at -100 mV Fig 5D).

Figure 6. Mechanistic insights in AF-mCPC after TGF-β1 treatment: The schematic depicts the molecular effects of TGF-β1 treatment on AF-mCPC: the binding of TGF-β1 with its receptors leads to the activation of SMAD2/3, which

translocates into the nucleus and activates the transcription of several genes involved in fibrosis and MFB differentiation (*i.e.* α-SMA, Col1A1, Col1A2). After the MFB differentiation, the cells produce and deposit collagen in the impaired tissue.

Table(s)

Click here to download high resolution image

Table 1. Clinical characteristics of patients included in the study

Patients Characteristics	CTR	AF	*p-value*
Number of patients	**11**	**11**	ns
Age (mean±SE)	70.2±2.2	67.1±2.5	ns
Male sex	6	5	ns
Valve Replacement			
Aortic Valve	11	4	<0,01
Mitral Valve	0	8	<0,01
Tricuspid Valve	1	8	<0,01
Cardiovascular risk factors			
Smoking	3	2	ns
Hypertension	6	8	ns
Dyslipidemia	6	3	ns
Diabetes	5	1	ns
previous AMI	1	1	ns
Obesity (BMI>30)	2	2	ns
#Pulmonary hypertension	3	5	ns
Medications			
Statins	3	1	ns
β-blockers	5	5	ns
Angiotensin II receptor antagonist	3	2	ns
ACE Inhibitors	3	3	ns

Figure 1

Click here to download high resolution image

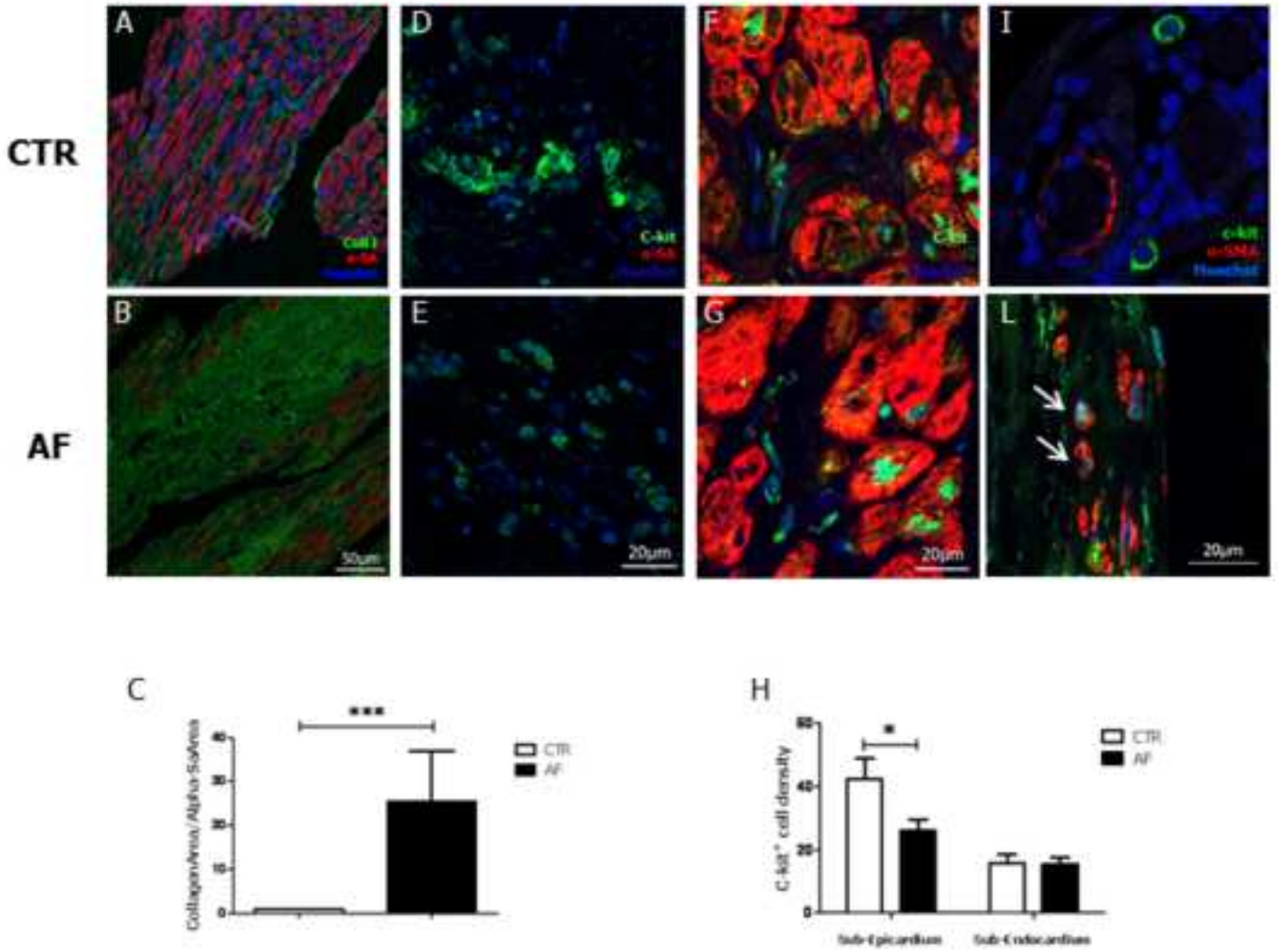

Figure 2

Click here to download high resolution image

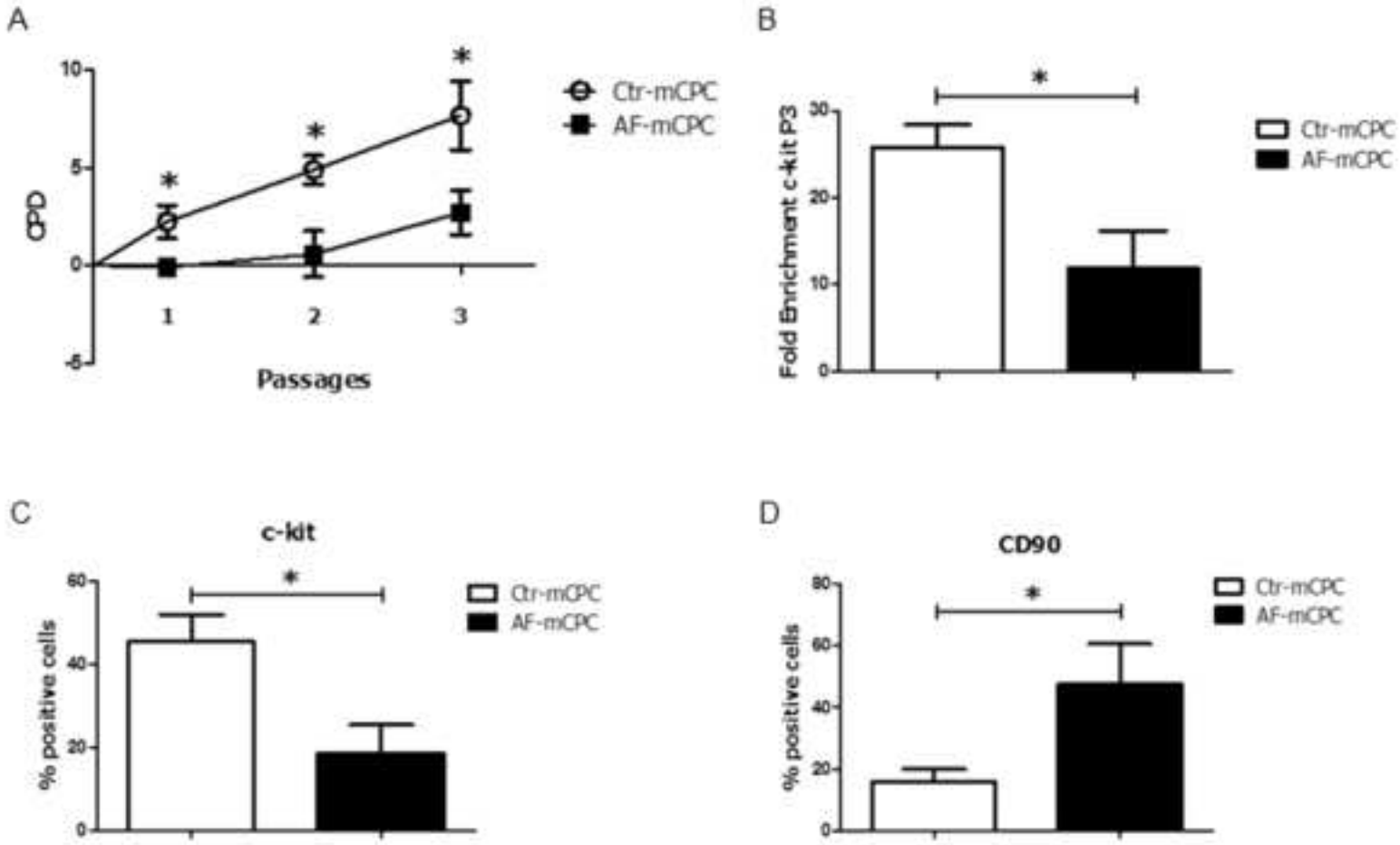

Figure 3

Click here to download high resolution image

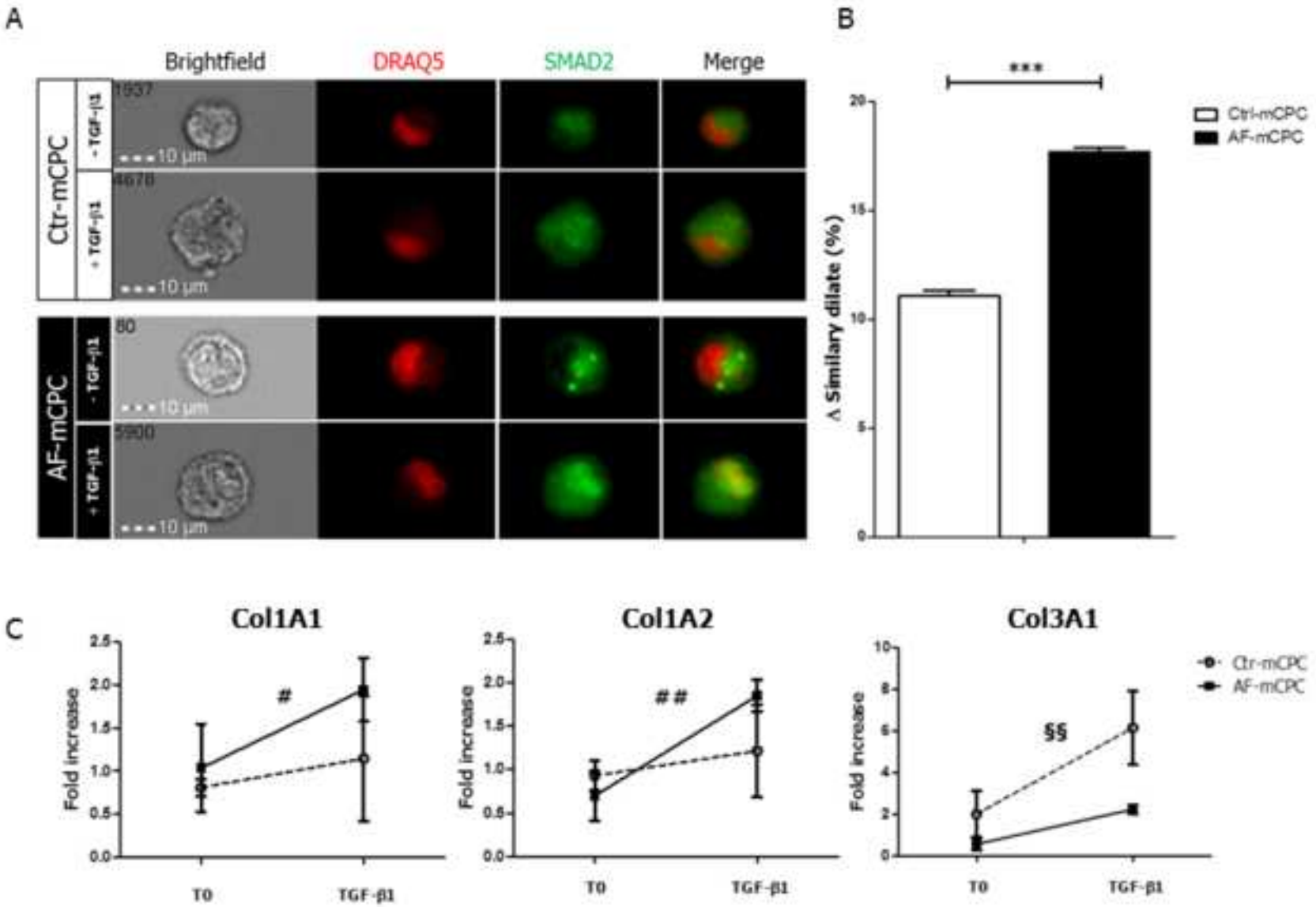

Figure 4

Click here to download high resolution image

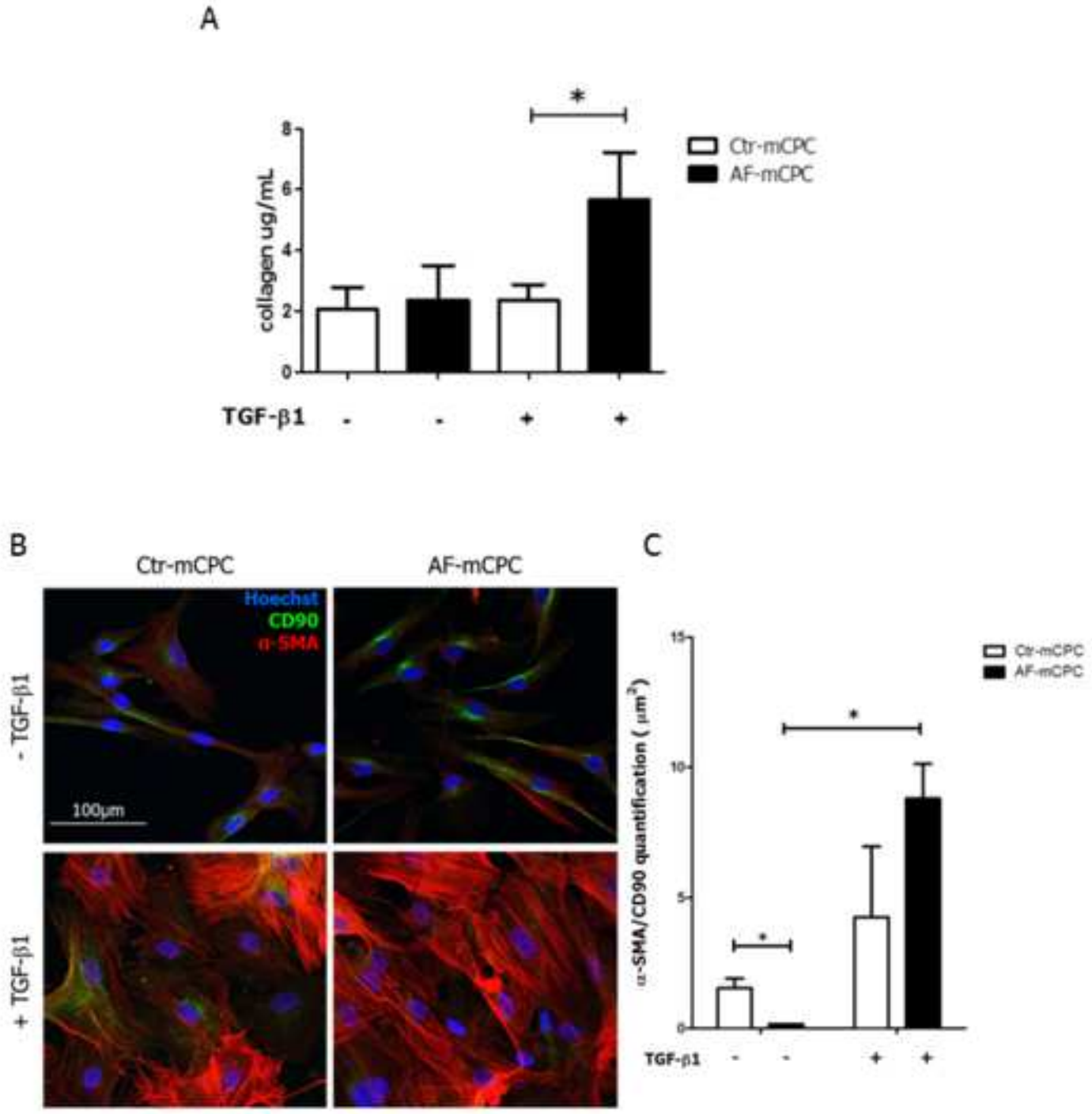

Figure 5

Click here to download high resolution image

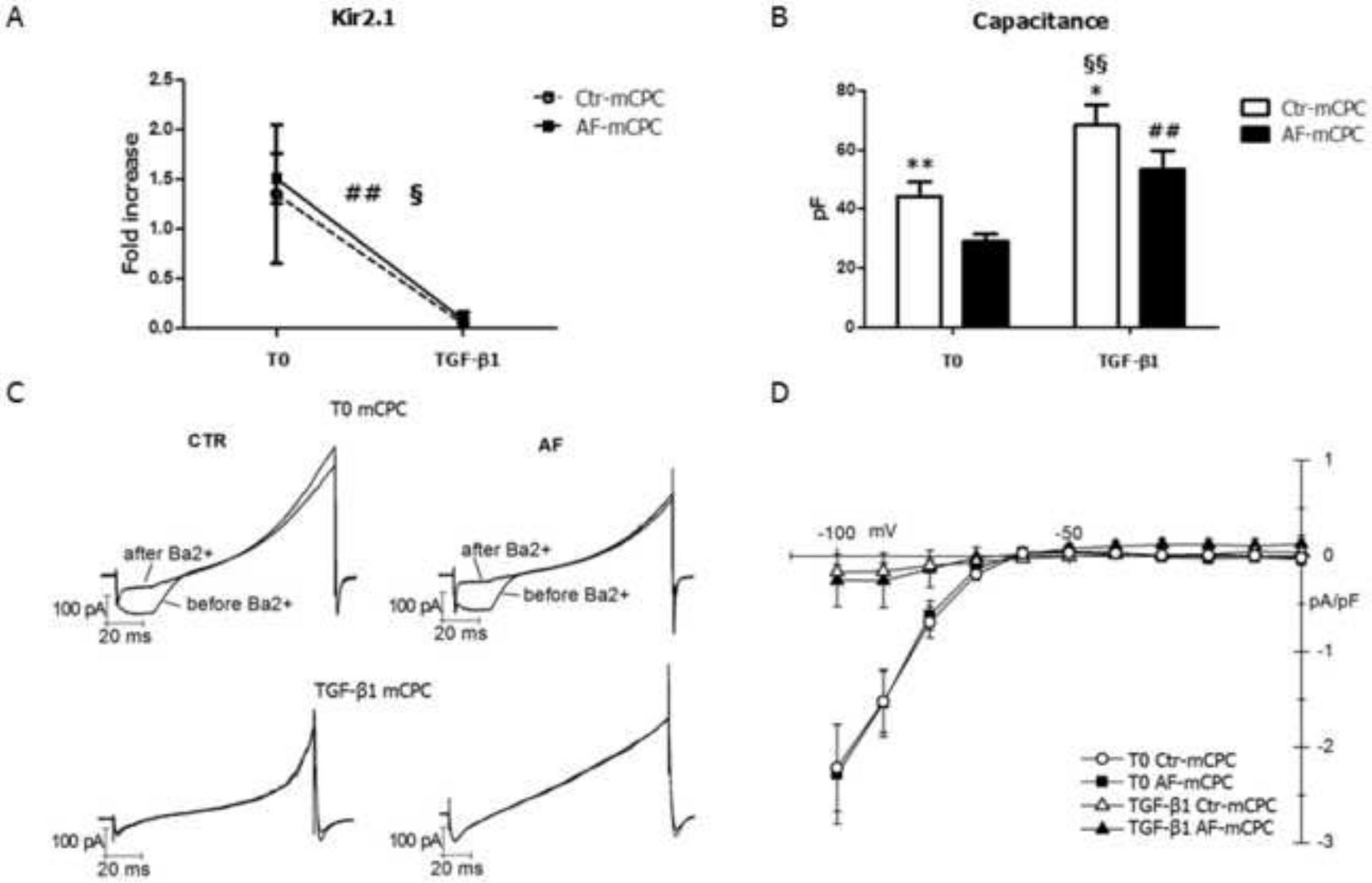

Figure 6

Click here to download high resolution image

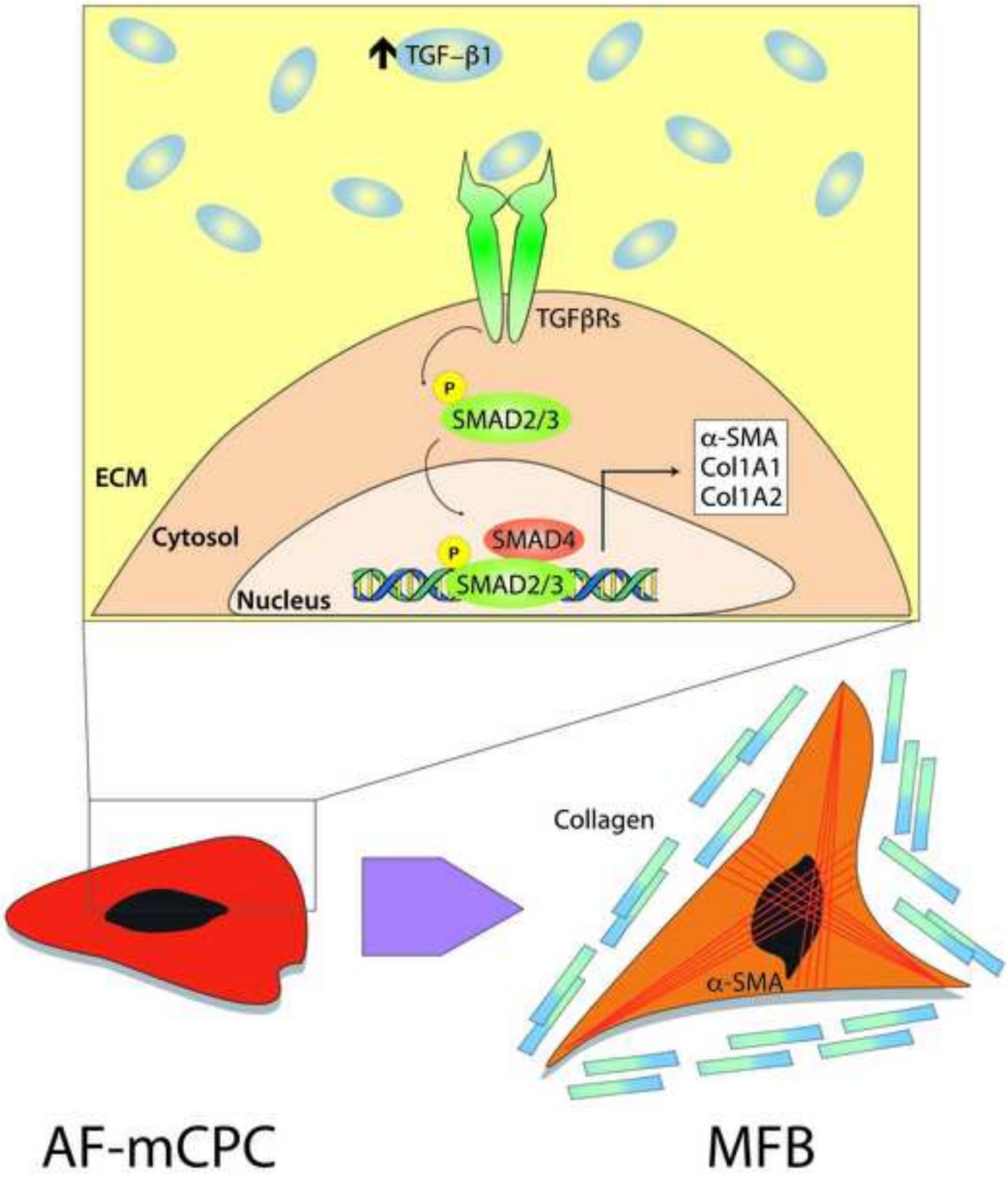

Supplemental Tables/Figures

Click here to download Supplemental Tables/Figures: Gambini et al Supplementary materials.docx